Title

Somatic Depdc5 deletion recapitulates electroclinical features of human focal cortical dysplasia type IIA

Journal

Annals of Neurology, 84(1)

ISSN

0364-5134

Authors

Hu, Shuntong
Knowlton, Robert C
Watson, Brendon O
et al.

Publication Date

2018-07-01

DOI

10.1002/ana.25272

Peer reviewed

HHS Public Access

Author manuscript

Ann Neurol. Author manuscript; available in PMC 2019 August 06.

Published in final edited form as:

Ann Neurol. 2018 July ; 84(1): 140–146. doi:10.1002/ana.25272.

Somatic *Depdc5* deletion recapitulates electro-clinical features of human focal cortical dysplasia type IIA

Shuntong Hu, MD[1,2], **Robert C. Knowlton, MD**[3], **Brendon O. Watson, MD, PhD**[4], **Katarzyna M. Glanowska, PhD**[2,5], **Geoffrey G. Murphy, PhD**[5], **Jack M. Parent, MD**[2,6], and **Yu Wang, MD, PhD**[2]

[1]Department of Neurology, the Third Xiangya Hospital, Central South University, Changsha, China

[2]Department of Neurology, University of Michigan, Ann Arbor, MI

[3]Department of Neurology, University of California San Francisco, San Francisco, CA

[4]Department of Psychiatry, University of Michigan, Ann Arbor, MI

[5]Molecular and Behavioral Neuroscience Institute, University of Michigan, Ann Arbor, MI

[6]Ann Arbor VA Healthcare System, Ann Arbor, MI

Abstract

Epileptogenic mechanisms in focal cortical dysplasia (FCD) remain elusive as no animal models faithfully recapitulate FCD seizures that have distinct electrographic features and a wide range of semiologies. Given that *DEPDC5* plays significant roles in focal epilepsies with FCD, we used *in utero* electroporation (IUE) with clustered regularly interspaced short palindromic repeats (CRISPR) gene deletion to create focal somatic *Depdc5* deletion in the rat embryonic brain. Animals developed spontaneous seizures with focal pathological and electroclinical features highly clinically relevant to FCD IIA, paving the way to understand its pathogenesis and develop mechanistic-based therapies.

INTRODUCTION

Focal cortical dysplasia (FCD) is a common cause of refractory focal epilepsies (FEs). As the most common underlying pathology in children with refractory FEs, it accounted for 26.8% of those cases in a series of approximately 2,600 specimens of brain tissue obtained during epilepsy surgery[1]. FCD has been classified into several subtypes and entities on the basis of histopathology. In particular, FCD II is an isolated lesion characterized by disrupted cytoarchitecture including dysmorphic neurons without (FCD IIA) or with balloon cells (FCD IIB) [1, 2]. Although FCD II is firmly linked to aberrant mTOR signaling

Corresponding Author: Yu Wang, M.D., Ph.D., Address: Department of Neurology, 5025 BSRB, 109 Zina Pitcher Place, Ann Arbor, MI, 48109-2200, Telephone: 734-936-1997, Fax: 734-763-7686, eegwang@med.umich.edu.

Author Contributions: Y.W. contributed to the conception and design of this study. All authors contributed to the acquisition and analysis of data. Y.W., J.M.P. and B.O.W. contributed to drafting the text.

Potential Conflicts of Interest: Nothing to report.

pathways[3], a major challenge in understanding its epileptogenesis and intractability is to develop animal models that recapitulate its genetics, pathology and electroclinical expression. For example, transgenic rodents, antimitotic agent and irradiation models lack a focal lesion. Freeze lesions produce circumscribed lesions but fail to capture its genetics and pathologies. Recently, focal pathology was replicated in mouse models using IUE to focally knockdown the mTOR inhibitor *Tsc1/2* or overexpress mutant mTOR activators[4]. However, a fundamental impediment to clinical translation is all these models didn't have focal electrographic signatures of human FCD seizures such as paroxysmal fast activity (PFA)[5], or fingerprints for the epileptogenic zone including low voltage fast activity (LVFA)[6]. While nearly all patients develop seizures with various semiologies, these FCD animals only displayed generalized tonic-clonic seizures (GTCs) and a significant number of them didn't develop spontaneous seizures[7].

The focal lesion seen in FCD II has led to the hypothesis that somatic mosaic mutations are the underlying genetic mechanism. Recent work has identified somatic activating mutations in MTOR itself, genes encoding positive regulators of MTOR, and new genes as negative regulators of MTOR via germline loss-of-function mutation coupled to demonstrated or inferred somatic loss of the second allele[8]. Germline or somatic *DEPDC5* mutations are increasingly recognized as the common cause of familial or sporadic FEs including monogenic entities such as familial focal epilepsy with variable foci (FFEVF), autosomal dominant nocturnal frontal lobe epilepsy (ADNFLE) or familial temporal lobe epilepsy[9]. In addition to its role in MRI-negative focal epilepsy, *DEPDC5* has also been associated with epileptogenic structural brain malformations, from FCD to large cortical malformations, such as hemimegalencephaly [8]. DEPDC5 is part of a complex named GAP activity toward RAGs (GATOR) complex 1 (GATOR1), together with the proteins NPRL2 and NPRL3. As a key member of the amino acid sensing machinery, GATOR1 complex functions independently of TSC1/TSC2 signaling and directly inhibits mTORC1 recruitment to lysosomal membranes[10]. However, no *DEPDC5*-related FEs animal model exists and all *Depdc5* transgenic animals reported to date failed to develop spontaneous seizures. All homozygous knockout animals died embryonically while heterozygous knockouts either showed no or subtle pathologies[11]. Although a neuron-specific *Depdc5* conditional knockout mouse survived to adulthood with severe neurological phenotypes, spontaneous focal electroclinical seizures were not recorded[11]. Given its significant role in FEs and unique function in the mTOR pathway, we performed IUE with CRISPR gene editing (CRISPR-IUE) on rat brains at embryonic day (E) 13–14 to introduce a focal region of somatic *Depdc5* deletion and generated animals with pathological and electroclinical expression highly similar to human FCD IIA.

METHODS

Plasmids, IUE and animals

Two *Depdc5* gRNAs were designed using an online program (http://crispr.mit.edu) as previously described, and subcloned into the PX330 vector (Addgene, plasmid 42230)[12]. *Depdc5*B was designed to target exon 12: 5′-GGTGGTGCAGAACGAGAGAA -3′, and *Depdc*5M was designed to target exon 8: 5′-GTTCCGTTCTACGTCGGCTA-3′. The

faithfulness scores were 95 and 98 respectively. pCAG-GFP, piggyBac donor plasmid (PBCAG-eGFP) and helper plasmid encoding piggyBac transposase (PBCAG-PBase) were obtained from Dr. Joseph LoTurco (University of Connecticut)[13]. IUE was performed on rats (Sprague-Dawley, Charles River Laboratories) as previously described[12]. The final concentration used for transfections were: 0.5 μg/μl for eGFP, 1.5 μg/μl for *Depdc5* CRISPR gRNA/Cas9. To track the entire lineage of transfected neural progenitors, PBCAG-eGFP (0.5 μg/μl) and pCAG-PBase (1 μg/μl) were co-electroporated with *Depdc5* CRISPR gRNA/Cas9. pCAG-eCas9-T2A-GFP-U6-gRNA plasmid (a gift from Jizhong Zou; Addgene plasmid # 79145) was used at 1.5 μg/μl. All animal studies were approved by the Institutional Animal Care and Use Committee of the University of Michigan.

Next Generation Sequencing

To estimate the rate of somatic *Depdc5* LoF mosaicism in the cortex, *Depdc5* CRIPSR-IUE transfected cortex was resected under the fluorescent dissection microscope. Targeted genomic areas flanking gRNA binding sites were PCR amplified using Platinum High Fidelity Taq DNA polymerase (Invitrogen, 11304–011). PCR products were sent for deep sequencing at the Center for Computational and Integrative Biology, Massachusetts General Hospital, Harvard. Primers used for targeted sequencing were forward 5′ CCTTGAAACGTTGTAATGAACCCGA, and reverse primer 5′TGACACACAGATGCAGTACCT.

Long-term EEG recording and analysis

To determine if rats that underwent *Depdc5* CRISPR-IUE exhibit electroclinical seizures and interictal epileptiform discharges (IEDs), we monitored animals with continuous video-EEG. Rats were implanted with four epidural screw electrodes at P60. Procedures for affixing electrodes were performed as previously described[14]. Four burr holes were made, and electrodes were positioned and fastened (left and right parietal, one cerebellar, and one reference posteriorly over the sinus cavity) using mounting screws (E363/20; PlasticsOne, Roanoke, VA). The sockets were fitted into a 6-pin electrode pedestal and the entire apparatus was secured with dental cement (Stoelting). One week after surgery, animals were monitored continuously for 3–14 days by video/EEG recording (Natus, Middleton, WI). Recordings were sampled at 4056 Hz and were analyzed offline with concurrent video. Seizures and epileptiform activity were assessed manually in their entirety by fellowship trained and board-certified epileptologists blind to experiments. IEDs are described as transients distinguishable from background activity with a characteristic morphology typically, but neither exclusively nor invariably, found in interictal EEGs of people with epilepsy. Epileptiform patterns have to fulfill at least 4 of the following 6 criteria: 1) Di- or tri-phasic waves with sharp wave or spike morphology (<200 msec duration); 2) Different wave-duration than the ongoing background activity; 3) Asymmetry of the waveform: a sharply rising ascending phase and a more slowly descending phase, or vice versa; 4) The transient is followed by an associated after-going slow wave; 5) The background activity surrounding epileptiform discharges is disrupted by the presence of the epileptiform discharges; 6) Distribution of the negative and positive potentials on the scalp suggests a source of the signal in the brain[15]. Seizures are defined as EEG phenomenon consisting of repetitive epileptiform EEG discharges at >2 cycles/second and/or characteristic pattern with

quasi-rhythmic spatio-temporal evolution (i.e. gradual change in frequency, amplitude, morphology and location), lasting at least several seconds (usually >10 s). Two other short duration (<10 s) EEG seizure patterns are defined as electrodecrement or low voltage fast activity seen during clinically apparent epileptic seizures. EEG seizure patterns unaccompanied by behavioral epileptic manifestations are referred to as electrographic or subclinical seizures[15]. For detection of sleep state, EEG voltage data was converted into a time-frequency power graph using a multi taper method at 1 second resolution. Each second was automatically classified into NREM or WAKE-like states based on bimodality tests of cortical signals as previously described[16]. Please see code in SleepScoreMaster.m file in GitHub repository: https://github.com/buzsakilab/buzcode.

Immunocytochemistry

Brains were removed and fixed in 4% paraformaldehyde in PBS after transcardial perfusion, sectioned at 50–80 μm on a vibratome (Leica VT1000S) and processed for immunocytochemistry as free-floating sections[12]. Primary antibodies included mouse anti-pS6 (1:2,000, Cell Signaling # 2211), chicken anti-GFP (1: 1,000, Aves GFP-1020), mouse anti-Nestin (1:20, Millipore clone rat-401), mouse anti-nonphorphorylated neurofilamin H (1: 200, Biolegend, clone#SMI32). Fluorescently conjugated secondary antibodies (AlexaFluor 488, 594 or 647) were obtained from Molecular Probes, and nuclei were labeled with Bisbenzimide (Molecular Probes H1398).

Brain slice preparation, electrophysiological recordings and data analysis

Male and female rats (P21–28) that previously underwent IUE at E13 were used for electrophysiological recordings. Slices were prepared as previously described[12]. Electrophysiological recordings were made in a recording chamber mounted on the stage of an upright microscope (customized Scientifica Optical Platform). Slices were continuously perfused (miniplus®3, Gilson, Inc.) with ACSF containing 1 μM tetrodotoxin (TTX), 20 μM 6-cyano-7-nitroquinoxaline-2,3-dione (CNQX) and 20 μM d(−)2-amino-5-phosphonovaleric acid (AP-5) to block action potential firing and ionotropic glutamate currents at a rate of 5–6 ml/min at 31–32°C (in-line heater TC-324B, Warner Instrument, Co.). GFP-expressing cells in cortical layers 2 and 3 were targeted for recordings. 3–5 MΩ resistance micropipettes were filled with an internal solution containing in mM: 100 Cs-gluconate, 0.2 EGTA, 5 $MgCl_2$, 40 HEPES, 2 Mg-ATP, 0.3 Na-GTP, 1mM QX-314, pH 7.2. Data were acquired at 20 kHz and filtered at 5 kHz. Only cells with stable passive properties were further analyzed. We collected data from a maximum of 3 neurons per animal to avoid bias. Statistical analysis was performed using Graphpad Prism (GraphPad Software, Inc.). Average values for each of the variables were calculated per cell and further averaged for each experimental group. Parametric and non-parametric statistical analyses were performed as dictated by data distribution.

Image acquisition, soma size measurements and statistical analyses

Multi-channel imaging was performed using a Leica SP5 confocal microscope. All the images were further processed in Adobe Photoshop CS3 software. The soma size of GFP+ neurons from P21~30 brains were compared between control and *Depdc5* CRISPR IUE animals. Automated measurement was performed in ImageJ. Statistical analysis was

performed using Microsoft Excel and GraphPad. ≥3 biological replicates were used for all studies. A confidence interval of 95% ($P<0.05$) was required for values to be considered statistically significant. All data are presented as mean±S.E.M. unless noted otherwise.

RESULTS

Phosphorylated ribosomal protein S6 (pS6) is commonly used as a marker of mTORC1 activity because mTORC1 activates p70 S6 kinase 1, which phosphorylates S6[10]. To examine mTORC1 hyperactivation, immunostaining for pS6 was performed on brain sections from 3-week-old rats that were co-electroporated with a *Depdc5* guide RNA (gRNA)/Cas9 construct and a green fluorescence protein (GFP)-encoding plasmid (Fig. 1a, b). After *Depdc5* CRISPR-IUE, pS6 immunoreactivity and soma size significantly increased in GFP-expressing neurons as compared to non-transfected overlying and adjacent cortex, opposite hemisphere (data not shown) and control CRISPR transfected brains (Fig. 1c–g). Interestingly, cell non-autonomous mTOR hyperactivation was observed in GFP-negative neurons with substantial extension to overlying and adjacent cortex, in line with clinical data that histological and electrographic abnormalities occur beyond MRI-visualized margins[17] (stars in Fig. 1c–f, arrowheads in Fig. 1e′, f′ and g). Antibodies to nonphosphorylated neurofilament proteins (SMI-32) revealed aberrant cytoplasmic accumulation of neurofilament proteins in the dysplastic cortex of *Depdc5* CRISPR-IUE rats (Fig. 1h), consistent with pathological findings observed in human FCD II [2]. However, Nestin-positive cells, a hallmark of balloon cells in human FCD IIB, were not observed in (Fig. 1i). These findings suggest that focal *Depdc5* somatic mutations in rat cortex generates human FCD IIA pathologies. Although we did not quantify the efficiency of *Depdc5* gRNAs, we and other groups have shown that IUE-CRISPR achieves gene knockout (KO) efficiency above 80%[12, 18]. The specificity of *Depdc5* deletion was confirmed by finding similar cellular and electrographic phenotypes using gRNAs targeting two different *Depdc5* exons (Fig. 1a). Specificity was further supported by pharmacological rescue experiments showing that treatment with the rapamycin analog Everolimus normalized soma size after *Depdc5* deletion (Fig. 1j, k). To estimate the degree of somatic Depdc5 loss of function (LoF) mosaicism, genomic DNA was extracted from the dysplastic cortex resected under fluorescent microscope. Targeted genomic areas flanking gRNA binding sites were PCR amplified and sent for next generation sequencing (NGS, >70,000 reads). The rate of Depdc5 LoF mosaicism ranged from ~2.64% to ~ 3.22 % (N=3). Whole-cell patch clamp recordings of acute cortical slices showed firing of doublet spikes and decreased input resistance in GFP-labeled cortical neurons with *Depdc5* deletion (Fig. 1l–m).

Critically, 100% (11/11 from more than 3 different litters) of rats undergoing *Depdc5* IUE-CRISPR developed frequent focal interictal epileptiform discharges (IEDs) and spontaneous seizures. IEDs (Fig. 2a–h) were restricted to the hemisphere with dysplastic tissue, in contrast to generalized discharges with current FCD models. Importantly, paroxysmal fast activity (PFA), rhythmic spikes, and periodic lateralized epileptiform discharges (PEDs), hallmarks of human FCD II [5], were detected in the rats as well as our FCD II patients (Fig. 2.a′–d′). High frequency oscillations (HFOs) was also lateralized to the lesional side, supporting focal epileptogenicity (Fig. 2h–j). IEDs were also highly sleep-dependent (Fig. 2k). Ictally, electrographic seizure onsets were lateralized to the lesional hemisphere, and the

common onset patterns in patients with FEs, including focal low voltage fast activity (LVFA), rhythmic spikes, background suppression and periodical epileptiform discharges (PEDs)[6], were frequently observed (Fig. 3a, c–d). These electrographic features were similar to those seen with intracranial ictal EEG recordings in FCD II patients and one patient with a pathological *Depdc5* mutation (Fig. 3b). Semiologically, the clinical seizure expression in rats, including behavioral arrest, tonic stiffening and contralateral clonic activity (Online videos 1–5), more closely recapitulates the variability seen in human FCD than existing models that show limited semiologies or only GTCs[7]. For example, behavioral arrest was commonly observed in these rats, similar to human complex partial seizures. Many seizures presented with subtle clinical/behavioral changes, such as waking up and subtle trunk tonic posturing. Generalized tonic-clonic seizures did occasionally occurred late into the seizure but never occurred at the onset.

DISCUSSION

To our knowledge, this is the first animal model that recapitulates genetics, pathology and most importantly, electroclinical features of human FCD IIA. We did not observe Nestin-positive balloon cells that are typically seen in human FCD IIB[3]. Considering the striking difference in neurogenesis between human and rodent, particularly the absence of outer radial glia cells in rodents[13], it is probably not a surprise that a rodent model lacks certain anatomical features. In addition, balloon cells have been shown to be silent electrographically[19]. Genetically, germline *DEPDC5* mutations occur more often than all other mutations in FE-related genes combined[9], and it directly inhibits mTOR independently of TSC1/TSC2 signaling[10]. Although *DEPDC5* somatic mutation has been associated with brain malformations from FCD to hemimegalencephaly [9], how a germline mutation sustains a focal pattern in inherited epilepsy still remains enigmatic. A plausible emerging hypothesis is that *DEPDC5* germline LoF mutation together with a second biallelic somatic hit in *DEPDC5* itself lead to the development of FCD, known as “two-hit” mechanism initially described in cancer and tuberous sclerosis[9]. This biallelic inactivation hypothesis is also supported by a recent report of a *DEPDC5* somatic nonsense variant in the resected brain tissue from an individual with FCD IIA and a familial history of focal epilepsy due to a germline mutation in *DEPDC5*[9]. Pathologically, both cell autonomous and cell non-autonomous mTOR hyperactivation were observed in our model, in line with the clinical observation that FCD histologic and electrographic abnormality occur beyond the MRI margin[17]. Clinically, our *Depdc5* CRISPR-IUE rats have a distinctly different electroclinical repertoire from current FCD models. The full spectrum of seizure semiologies and characteristic interictal and ictal discharges are unique and highly clinically relevant to human FCD. However, two important questions remain to be answered. First, cell non-autonomous mTOR hyperactivation, a surprising finding, likely plays an important role in epileptogenesis and overall clinical manifestations. However, the mechanism is completely unknown. Second, interneurons are firmly tied to ictogenesis and epileptogenesis in FCD[20]. However, they are born in the ventral medial ganglionic eminence (MGE) and lateral ganglionic eminence (LGE)[21] that are not transfected by *Depdc5* CRISPR-IUE. A unifying hypothesis would be that cell non-autonomous mTOR hyperactivation impairs

interneuron development. Our model should pave the way to study epiletogenesis and ictogenesis at cellular and circuit levels, as well as to develop mechanistic-based therapies.

Supplementary Material

Refer to Web version on PubMed Central for supplementary material.

Acknowledgments

Y.W. received funding from NIH-NINDS(K08NS099379), Pediatric Epilepsy Research Foundation and Citizens United for Research in Epilepsy. J.M.P. received funding from NIH-NINDS (R01NS058585). G.G.M. received funding from NIH-NIA (R01AG052934). K.M.G. received funding from American Epilepsy Society. B.O.W. received funding from NIH-NIMH (K08MH107662). R.C.K received funding from NIH-NINDS (U01NS09871). S.H. received funding from China Scholarship Council (201606370207).

References

1. Blumcke I, et al. Histopathological Findings in Brain Tissue Obtained during Epilepsy Surgery. N Engl J Med. 2017; 377(17):1648–1656. [PubMed: 29069555]
2. Blumcke I, et al. The clinicopathologic spectrum of focal cortical dysplasias: a consensus classification proposed by an ad hoc Task Force of the ILAE Diagnostic Methods Commission. Epilepsia. 2011; 52(1):158–74. [PubMed: 21219302]
3. Iffland PH 2nd, Crino PB. Focal Cortical Dysplasia: Gene Mutations, Cell Signaling, and Therapeutic Implications. Annu Rev Pathol. 2017; 12:547–571. [PubMed: 28135561]
4. Becker AJ, Beck H. New developments in understanding focal cortical malformations. Curr Opin Neurol. 2017
5. Quirk JA, et al. EEG features of cortical dysplasia in children. Neuropediatrics. 1993; 24(4):193–9. [PubMed: 8232776]
6. Grinenko O, et al. A fingerprint of the epileptogenic zone in human epilepsies. Brain. 2017
7. Lim JS, et al. Somatic Mutations in TSC1 and TSC2 Cause Focal Cortical Dysplasia. Am J Hum Genet. 2017; 100(3):454–472. [PubMed: 28215400]
8. D'Gama AM, et al. Somatic Mutations Activating the mTOR Pathway in Dorsal Telencephalic Progenitors Cause a Continuum of Cortical Dysplasias. Cell Rep. 2017; 21(13):3754–3766. [PubMed: 29281825]
9. Marsan E, Baulac S. mTOR pathway, focal cortical dysplasia and epilepsy. Neuropathol Appl Neurobiol. 2018
10. Bar-Peled L, et al. A Tumor suppressor complex with GAP activity for the Rag GTPases that signal amino acid sufficiency to mTORC1. Science. 2013; 340(6136):1100–6. [PubMed: 23723238]
11. Yuskaitis CJ, et al. A mouse model of DEPDC5-related epilepsy: Neuronal loss of Depdc5 causes dysplastic and ectopic neurons, increased mTOR signaling, and seizure susceptibility. Neurobiol Dis. 2018; 111:91–101. [PubMed: 29274432]
12. Wang Y, et al. Critical roles of alphaII spectrin in brain development and epileptic encephalopathy. J Clin Invest. 2018
13. Pollen AA, et al. Molecular identity of human outer radial glia during cortical development. Cell. 2015; 163(1):55–67. [PubMed: 26406371]
14. Korn MJ, Mandle QJ, Parent JM. Conditional Disabled-1 Deletion in Mice Alters Hippocampal Neurogenesis and Reduces Seizure Threshold. Front Neurosci. 2016; 10:63. [PubMed: 26941603]
15. Nick Kane JA, Benickzy Sandor, Caboclo Luis, Finnigan Simon, Kaplan Peter W, Shibasaki Hiroshi, Pressler Ronit, Michel JAM, van Putten. A revised glossary of terms most commonly used by clinical electroencephalographers and updated proposal for the report format of the EEG findings. Revision 2017. Clinical Neurophysiology Practice. 2017; 2:170–185.
16. Watson BO, et al. Network Homeostasis and State Dynamics of Neocortical Sleep. Neuron. 2016; 90(4):839–52. [PubMed: 27133462]

17. Schwartz TH. Cortical dyplasia: complete resection correlates with outcome … But, complete resection of what? Epilepsy Curr. 2009; 9(4):100–2. [PubMed: 19693325]
18. Chen F, et al. Tracking and transforming neocortical progenitors by CRISPR/Cas9 gene targeting and piggyBac transposase lineage labeling. Development. 2015; 142(20):3601–11. [PubMed: 26400094]
19. Cepeda C, et al. Are cytomegalic neurons and balloon cells generators of epileptic activity in pediatric cortical dysplasia? Epilepsia. 2005; 46(Suppl 5):82–8. [PubMed: 15987258]
20. Calcagnotto ME, et al. Dysfunction of synaptic inhibition in epilepsy associated with focal cortical dysplasia. J Neurosci. 2005; 25(42):9649–57. [PubMed: 16237169]
21. Hu JS, et al. Cortical interneuron development: a tale of time and space. Development. 2017; 144(21):3867–3878. [PubMed: 29089360]
22. Carvill GL, et al. Epileptic spasms are a feature of DEPDC5 mTORopathy. Neurol Genet. 2015; 1(2):e17. [PubMed: 27066554]

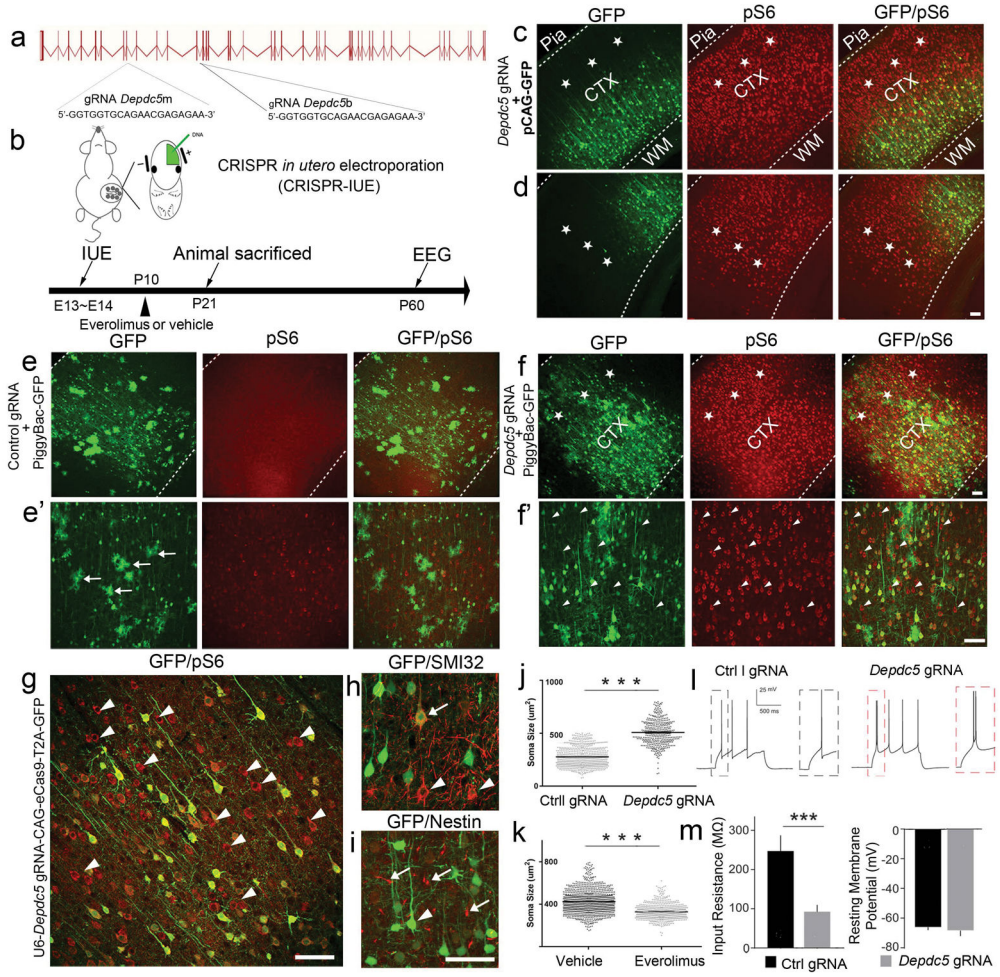

Figure 1. *Depdc5* CRISPR-IUE leads to focal cortical mTOR hyperactivation

a) Two short guide RNAs (sgRNAs) are used to target rat *Depdc5* either at exon 8 or exon 12. b) CRISPR-IUE experiments are performed at E13–14. Animals are euthanized at P21 for pathology evaluation or are treated with Everolimus for 11 days beginning at P10. Video-EEG monitoring starts at P60. c-d) Co-electroporation of pCAG-GFP and *Depdc5* CRISPR significantly increases pS6 immunoreactivity in both GFP+ and GFP− cells. Stars indicate cell non-autonomous mTOR hyperactivation in the overlying (c) and adjacent cortices (d). To show that increased p-S6 in GFP-negative cells is not due to dilution of episomal GFP transfection by dividing cells, *Depdc5* CRISPR was co-electroporated with a Piggybac transposon system encoding GFP (see method) that integrates into the genome of neural progenitors. e) in control CRISPR-transfected brains, baseline pS6 immunoreactivity is minimal while f) In *Depdc5* CRISPR-transfected brains, pS6 expression still markedly increases in both GFP-positive and GFP-negative cells. e′) higher magnification images of e). GFP labeled glial cells (arrows) suggest successful genome integration of GFP plasmid. f ′) higher magnification images of f). Many GFP-negative cells show strong pS6 immunoreactivity (arrowheads), suggesting cell non-autonomous mTOR hyperactivation. g) Because plasmid co-transfection efficiency is not 100%, GFP-/pS6+ positive neurons could be neurons transfected with only *Depdc5* CRISPR plasmid. To ensure that all neurons

undergoing *Depdc5* CRISPR deletion are labeled with GFP, we electroporated a single vector plasmid that encodes eCAS9, *Depdc5* gRNA and GFP. With this approach, increased pS6 is still observed in GFP-negative cells (arrowheads), indicating cell non-autonomous mTOR hyperactivation. h) Antibody to a non-phosphorylated neurofilament protein (SMI-32) reveal aberrant cytoplasmic accumulation in both GFP(arrows) positive and negative neurons (arrowheads). i) Positive filamentous Nestin (arrows) staining, a typical pattern in reactive astrocytes, is seen in the dysplastic cortex. However, balloon cells, a pathological hallmark of FCD IIB, that show patchy and accumulated Nestin staining in the cell body, is never seen in *Depdc5*-CRISP transfected brains. An arrowhead here indicates that a hypertrophic GFP positive cell is negative for Nestin staining. j) The soma size of *Depdc5* CRISPR-transfected neurons (N=3 rats, n=412 cells) is nearly doubled vs. control cells (N=3, n= 715). Two-tailed *t* test, p=0.002. k) Postnatal administration of Everolimus partially rescues cytomegalic neurons. Drug group: N=3, n=661; No drug vehicle group: N=3, n=1096. Two-tailed *t* test, p=0.005. l) All cortical neurons with *Depdc5* deletion fire initial doublet action potentials (none in control), suggesting increased intrinsic excitability, and m) show decreased input resistance. N=3 rats, two-tail t-test. $p<0.05$. Scale bar: 100 μm.

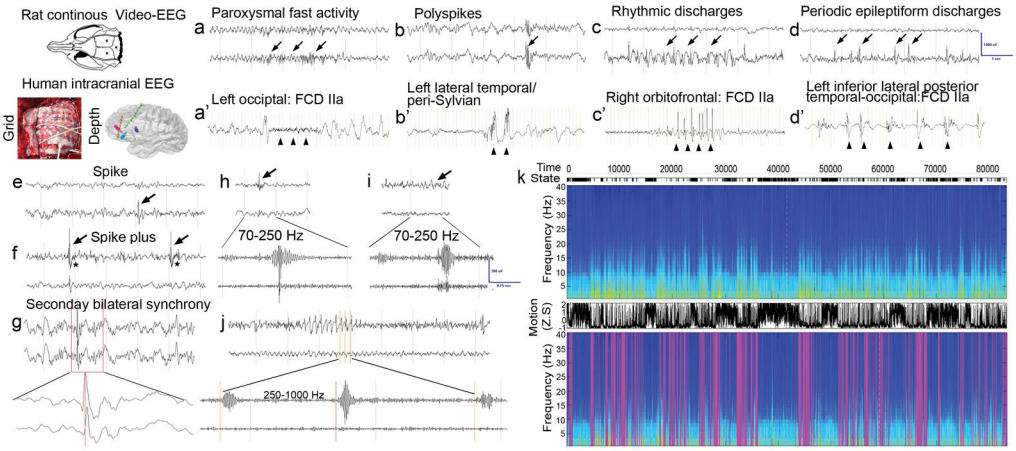

Figure 2. Interictal discharges highly resemble human FCD

For all rat EEG recordings, the upper trace is from electrode implanted in the right parietal head region and the lower trace is from the left (see method). Interictal EEG recordings from rats with *Depdc5* CRISPR-IUE, including PFA (a), polyspikes (b), rhythmic spike discharges (c), and PEDs (d) are lateralized to the lesional hemisphere, and are highly similar to intracranial subdural or depth EEG recordings from patient with FCD IIa including one with a *DEPDC5* mutation (p.Tyr281Phe)[22] (a′-d′). For all human intracranial recordings, shown is one electrode recording that captures the most representative EEG discharges. Other typical focal IED examples including e) single focal spikes, f) spikes with overriding fast activity (stars) with minimal electrical field to the opposite hemisphere. g) rapid bilaterally synchronous-appearing IEDs are seen occasionally but they display lateralized onset based upon asymmetric amplitude and lead-in time (red vertical line). h) ripples associated with a spike are displayed with 70–250 Hz frequency band. i) Ripples that are not associated with spikes. j) fast ripples associated with a train of spike-and-wave discharges are displayed with 250–1000 Hz frequency band. These HFOs are also lateralized to the lesional hemisphere. k) Shown is a spectrogram of oscillatory power (color) versus time (horizontal) across various frequencies at each time point (vertical). IEDs, shown as purple lines in the lower power spectral image occur predominatly in NREM sleep, recognized by increased lower frequency band power and lower motion scores - see upper panel for fully visible spectrogram, and see methods. To quantify IEDs during sleep vs. wakefulness, IEDs were counted during one hour of sleep and wakefulness for 3 days from 3 rats with *Depdc5* CRISPR-IUE. The average number of IEDs is 32.89 ± 6.326 during sleep, and 7 ± 3 during wakefulness (Two tailed t-test, p=0.002).

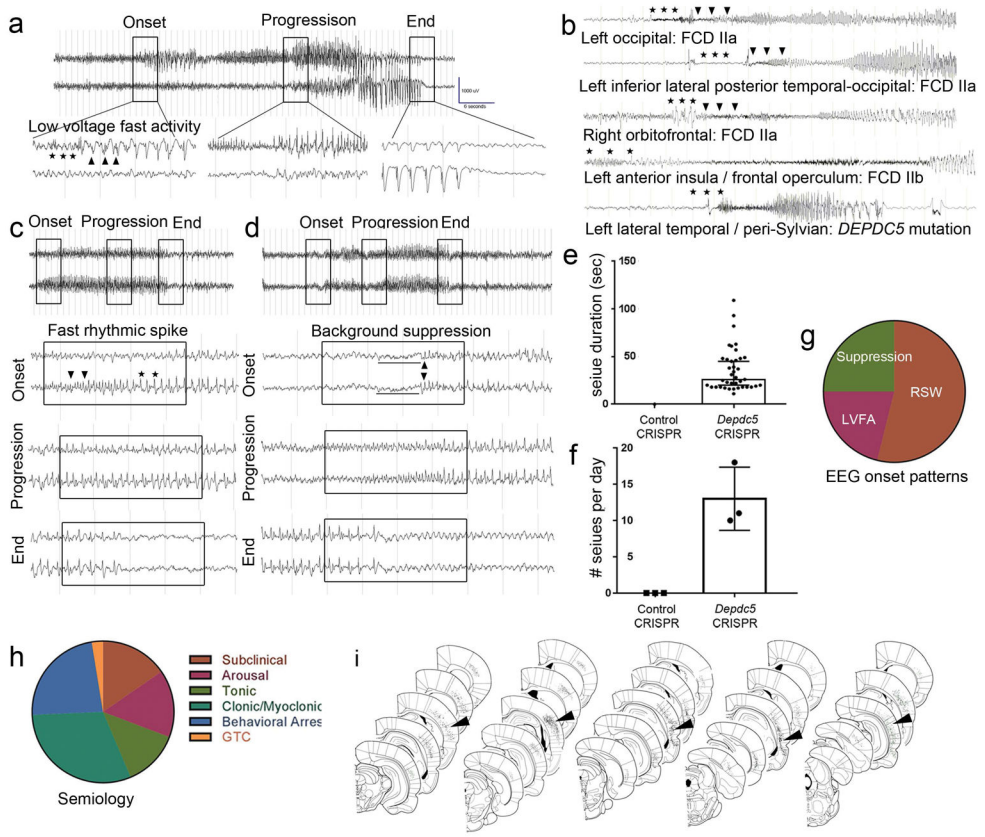

Figure 3. Electroclinical seizures highly resemble human FCD

a) shown is an entire seizure from a rat with *Depdc5* CRISPR-IUE. The top EEG traces have a compressed time-base of 5 mm/s, and the lower ones have a standard time-base of 30 mm/s. The seizure starts with fast rhythmic spikes at low voltage fast activity (LVFA) (stars) followed by 2–3 Hz spike and wave discharges (arrowheads). b) intracranial recordings from patients with FCD II show common ictal onset patterns including low voltage fast, background suppression and burst of rhythmic spikes. c–d) two additional representative seizures recorded from rats with *Depec5* CRISRP-IUE show typical seizure onset patterns in c) rhythmic spikes and d) background attenuation. e–h) 39 seizures from 3 different animals were analyzed for seizure duration (e; 35.97 ± 22.85s, median=26s), frequency (f; 13 ± 2.5/24 hr), EEG onset patterns (g) and semiology (h). The majority of seizures started with rhythmic spike discharges (RSW: 53.8%), background suppression (25.0%) and low voltage fast activity (LVFA: 21.2%). Behaviorally, most seizures showed clonus/myoclonus (30.1%) or behavioral arrest (e.g., freezing, stopping exploration) (23.1%). Other types included tonic posturing (12.8%) and arousal without other clear clinical signs (15.1%). 15.1% of electrographic seizures were subclinical. Notably, only one seizure progressed to a generalized tonic-clonic seizure. i) representative reconstructed brain sections showing the size and position of *Depdc5* CRISPR transfection (each black dot is a transfected neuron) at 5 rostro-caudal levels in 5 rats after EEG recording was completed at P70–90. Arrowheads indicate the section in each series with the most extensive *Depdc5* CRISPR transfection.